

# Effective Use of Scanning Laser Doppler Vibrometers for Modal Tests

Ben Weekes and David Ewins, University of Bristol, Bristol, UK

Vibration measurement using a scanning laser Doppler vibrometer (SLDV) has a number of advantages over the use of accelerometers – setup is rapid, the sensor is non-contacting, and many more measurement points can be acquired in a given testing period. Use of SLDVs can therefore drastically reduce concerns of spatial aliasing and makes identification of local modes simple. However, effective use of SLDVs for modal testing (or experimental modal analysis – EMA) can be difficult given that line of sight between the SLDV head and the tested surface must be maintained so significant parts of the structure may be unrepresented in the process. This has been addressed in recent trials of hybrid accelerometer/SLDV test geometries applied to aerospace structures, where a relatively sparse accelerometer array is combined with detailed SLDV inspections of local regions.

The laser Doppler vibrometer (LDV) is a type of optical interferometer that measures velocity at a point on a surface by detection of the Doppler shift of light – a phenomenon in which back-scattered (or reflected) light is frequency shifted if the emitting/reflecting body is moving relative to the source/viewer of the light. The laser notionally emits light at a single frequency, so by mixing the returned light with a reference monochromatic light source on a photo detector, a beat signal that can be measured with an extremely high accuracy is produced. The demodulated output takes the form of a voltage proportional to the measured velocity.

As an optical sensor, there are a number of differences in the application of LDV compared with transducers that are attached to a test piece. First, note that the laser potentially exists in a different inertial frame to the test piece. That is, relative vibration of either the LDV or the test piece will be detected. This can be problematic, since the LDV is usually mounted on a tripod that contacts the floor, while in a modal test, the test piece is often isolated on a soft suspension.

There are also potential optical issues: adequate laser light must be returned to the photo-detector for the demodulation electronics to function or else a “dropout” occurs where the output velocity signal becomes spurious and strongly negative (tending toward full-scale low) occurs. This issue is compounded by the issue of laser speckle.<sup>1,2</sup> Surfaces that are optically rough (non-specular) will see the laser light incident upon the surface self-interfere, which given the highly monochromatic and coherent content causes localized bright and dark regions. The speckle pattern observed is a spatial phenomenon, so the usual means to achieve a measurement when a dark speckle is incident upon the photo detector is simply to fractionally move the laser spot so that a brighter part of the speckle pattern is then incident upon the sensor.

The scanning LDV (SLDV) is an LDV with the addition of a pair of scanning mirrors and, typically, a video feed. For each test configuration, a calibration is performed so that the laser spot can be located on the surface of the test piece by interaction with the video feed. The scanning mirrors allow the laser to be steered, moving the measurement location. However, there must be line of sight between the mirrors and all desired measurement locations, limiting the scope of the test that can be performed by a single SLDV head in a single location. It is possible to use additional mirrors to expand the possible area of inspection, but movement of the mirrors will also be measured. Note that multilaser vibrometer systems are a subject of developmental interest.<sup>3</sup>

Like LDVs, SLDVs comprise a single sensor, and although data

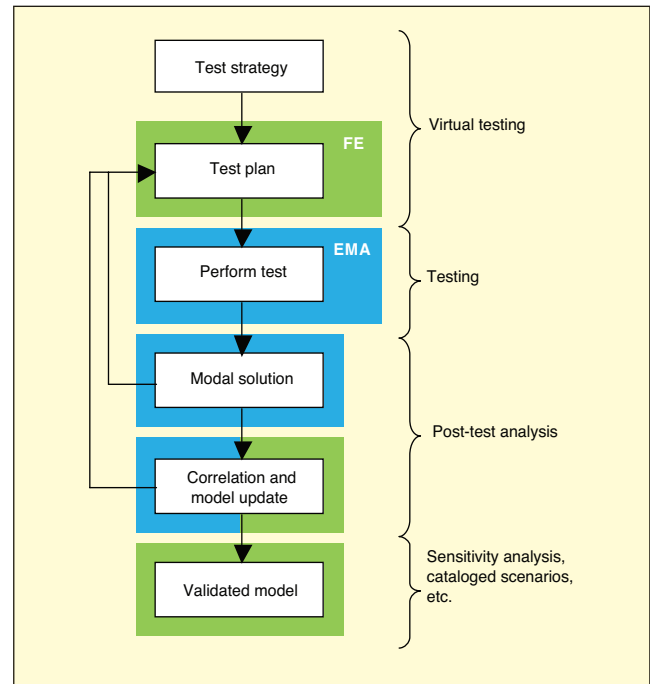


Figure 1. Schematic of complete model validation procedure, showing flow from virtual testing to a validated model, with the contributions from model and experimental analysis (green and blue respectively).

can be acquired at many locations, the measurements are sequential. The apparent timesaving from use of SLDVs and the increase in the number of measurements that can be taken are by virtue of how rapidly an SLDV can be set up compared to an array of physically attached transducers and their associated wiring. Since the SLDV measurement is sequential, the full excitation signal must be repeated at each measurement location (with repeat measurements as necessary); so for the SLDV measurement locations to be compared, the test should either be repeatable or statistically rigorous.

## Using SLDVs in Modal Analysis

A flowchart for a typical modal test appears in Figure 1, showing the often-iterative nature of the validation process. Virtual testing (or pretest) comprises test strategy and test plan, which can be summarised as “what test?” and “how?”<sup>4</sup> A finite-element (FE) model is used to aid test planning, helping to define specific aspects of the test, particularly regarding optimal locations for degrees of freedom (DOFs) for the frequency bandwidth of interest.

An experimental modal analysis (EMA) is performed as prescribed by the test plan, for which a modal solution is calculated. Given that the FE model used to generate the test plan is not validated, it is not surprising that the modal analysis may fail to describe the dynamics of the structure adequately at the first pass, so a new test plan and further experimental analysis may be required. Once an acceptable modal solution is believed to have been found, the FE model can be correlated against the EMA, and attempts can be made to update the model.

Again, the model updating process can fail if the model cannot be reconciled with the experimental data, requiring that revisions be made to the model structure, which in turn may show some deficiencies in the EMA. Once a model that accurately approximates the observed dynamics of the part or structure has been found and successfully updated, the model can be considered valid within the

Based on a paper presented at IMAC XXXII, the 32nd International Modal Analysis Conference, February 3-6, Orlando, FL, 2014.

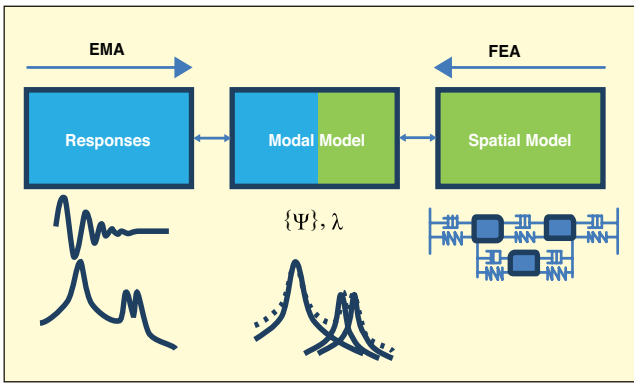


Figure 2. Schematic of modal analysis models.

bounds of the test (within stated frequency and amplitude ranges, at a given temperature, etc.) and can be used in rigorous predictive analyses. This would be too expensive to perform experimentally.

The SLDV is a transducer that yields data much like an accelerometer (albeit measuring velocity, not acceleration), but as discussed above in modal analysis we seek a dataset that describes the system dynamics fully. The SLDV allows many measurement locations to be captured, but redundant capture may not benefit modal analysis. In this section, test planning for SLDVs is discussed, and the fundamental line-of-sight limitation is addressed by use of a combination of SLDV and accelerometers. Also discussed is how to combine and import these hybrid datasets into existing modal analysis software.

### Changes to Test Design

The differences between performing an ad hoc experimental analysis and an EMA can be somewhat subtle but are informed by the ultimate use for the data. In Figure 2, the models through which the data move are shown schematically; measurements capture responses to an input from which data a modal description (solution) is found. The FE model is a spatial description of the test article, from which a modal solution can also be found, allowing the EMA and FE data to be correlated and model updating to be performed. The EMA and FE datasets are fundamentally mismatched since the EMA will typically comprise tens to hundreds of DOFs, while the FE model could easily comprise many thousands to millions of DOFs. Most often, the FE model is reduced to match the EMA rather than interpolation/extrapolation to expand the EMA dataset.

When updating the model, the EMA geometry defines the reduced FE geometry; that is, the number, orientation and distribution of the degrees of freedom. The test plan for the EMA is therefore more nuanced than an ad hoc experiment-only analysis of vibration, with a complete modal description usually sought such that the system equations are not under-determined by an inadequate choice of measurement degrees of freedom. Therefore, it is advised to use virtual testing wherever possible to guide non-trivial EMA. However, there is some difficulty in creating a practical SLDV test geometry using virtual test tools because of the additional constraint in measurement locations required to maintain line of sight.

Further, once an obtainable SLDV test geometry has been created in the virtual test software, it is difficult to then perform measurements at the prescribed measurement locations without resorting to manually programming the locations at length. Without further development of tools to ease this process of creating and performing an SLDV test based on a pre-test, the speed advantage of SLDVs is limited. An alternative approach would be simply to define many measurement locations so that there is no concern of spatial aliasing between modes; the pre-test and test geometries need not be identical in this case if sufficient measurement locations are defined. The limitation of this approach is that a single viewpoint of the laser for non-2D (non-planar) test objects will often fail to adequately capture the dynamics of the structure, necessitating supplementary transducers to provide additional DOFs out of the line of sight of the SLDV. The caveat in the use of additional transducers in such a manner is that the metrics on which the correlation is based will

(by default) be significantly weighted by the many SLDV points, so the relative weight of the supplementary DOFs (which are clearly of importance to be warranted) is reduced.

The capture of many non-coincident measurement locations using the SLDV inherently increases capture of local modes. The identification of local modes is usually an advantage of using the SLDV, since it is often desirable to update the model based only on the lower-order global modes, discarding the modes identified as local. This is because the low-order global modes are more likely to be a structural concern, and local modes often feature only subassemblies, which are likely to be subject to a boundary condition comprised of joints that are difficult to model (and therefore likely to be updated in a spurious way, to the detriment of the more important global modes). In the model updating process, the model is iteratively updated multiple times, making it easier to discard the EMA local modes and to rely on the FE local modes not correlating against the EMA global modes, therefore not affecting the model update.

### Import of SLDV Data – The Universal File Format

Modal analysis of structures that behave in a strongly linear manner is highly developed, with a number of software suites available in which to perform capture (LMS Test.Lab, DataPhysics SignalCalc, m+p international SmartOffice) and analysis (LMS Test.Lab, DataPhysics SignalCalc, Spectral Dynamics STAR Modal, HBM nCode, m+p international SmartOffice, Dynamic Design Solutions FEMtools) of the relevant data. However, these capture suites tend to require an array of transducers such that concurrent capture can be performed at all DOFs. Since capture is performed on discrete transducers by means of a simple voltage input, these systems can easily accommodate various transducers such as accelerometers and strain gauges. Such software suites currently lack the means to acquire data from SLDVs, which is not surprising, since interfacing with SLDVs requires calibration of the scanning mirrors to the video feed (calibration is test-specific), defining the scan geometry on the video feed, measurement sequencing, etc., with the hardware/software giving interface difficulties. The software that comes with SLDV systems is usually adequate to perform a test and to review the results as FRFs, ODSs and sometimes as mode shapes, damping values, etc., but for more detailed analyses it is often desirable to output the captured time histories or FRF data to perform the modal analysis in proven modal analysis software.

**Origin of Universal File Format.** The standard means of conveying modal test data is the universal file format (often .unv, .uff, .asc), an ASCII-based (text) format defined by the Structural Dynamics Research Corporation (SDRC)<sup>5</sup> in the late 1960s and early 1970s to permit transfer of data between early computer design and test systems. Such is the legacy of the format that the data fields are typified by 80-character limits to fit 80-column punch card records. As an ASCII-based format, the files can be opened with any text editor, and with the appropriate formatting guide, the files can be understood by a human operator.

**Important UFF Datasets for Modal Analysis.** Universal files comprise datasets of various types.<sup>5</sup> There is provision for time history and FRF data in dataset Type 58, and mode shape data in dataset Type 55. Also present in universal files are datasets containing the header information (metadata), units, geometry, and coordinate systems. In exporting data from one software package to another using universal files, it is often necessary to adjust the data manually if there is some disparity between the universal file interpretations for the software packages.

Despite the supposed standardization offered by the format, there is some ambiguity and variation in how the UFF interpreters are written. (For example, translation and rotation matrices may be defined to map from global to local coordinate systems, or vice versa.) There are also legacy dataset types that can lead to difficulties with incomplete support (geometry dataset Type 2411 vs. Type 15). Units are often imported incorrectly, especially in the case of units of acceleration (g, instead of mm/sec<sup>2</sup> when the units dataset specifies SI units). We have found cases of FRF plots scaled correctly in the modal analysis software, since the SI units in the axes labels were taken from the universal file, while

subsequent processing of the data in the same software package assumed units in g. Depending on the tools available in the modal analysis software and the permitted access to the underlying data, error-checking the imported data can be difficult, so such errors may go unnoticed.

**UFF and SLDV.** The strength of the universal file format is its widespread use and the relative simplicity in directly interrogating the files when troubleshooting. However, when dealing with many DOFs (as is typical for SLDV data) the files can become unwieldy and difficult to edit. The files can also become large, although the more recent binary dataset 58b can reduce file sizes. There is no fundamental incompatibility between UFF files and SLDV data. The difficulties stem from managing the increased amount of data from the multitude of SLDV measurement points and in combining datasets from various capture systems of supporting transducers (see next section).

### Managing Hybrid Datasets

As is described in the following case study, we have tended to use hybrid accelerometer-plus-SLDV datasets. This requires some management of the respective accelerometer and SLDV datasets, which are generated by two different capture systems. As such, both datasets have their own node numbering and coordinate systems, and capture different temporal derivatives. Additional complexity is often incurred, since most SLDV systems lack range finding and so assume all measurement points lie on a plane, with the measurement perpendicular to the plane (see next section). A simple program was written to combine the datasets, taking the following approach:

- Take an accelerometer coordinate system as the master (often there is only one coordinate system defined), and by means of three or more reference points common to both datasets, map the SLDV coordinates into the accelerometer system (using Reference 6).
- Define local coordinate systems for all SLDV points to reorient each measurement axis to the incident angle of the laser. This requires the assumption that the test-piece is relatively planar and an approximate location for the SLDV. This assumption is acceptable when the stand-off between the SLDV and test piece is large relative to the geometric complexity of the test object in the stand-off direction.
- Scale the velocity FRF data to acceleration by a divisor of  $j\omega$ , (linearity is assumed) and so a general solution of the type  $x(\omega) = A \exp(j\omega t)$  corresponds to  $x = v/(j\omega) = a/(j\omega)^2$ .
- Append SLDV data to the accelerometer data, correcting node numbering (and associated references such as coordinate systems, driving point(s), etc.).

The UFF output of commercial software requires some options regarding definition of the coordinate systems, units, and legacy UFF dataset formats depending on the modal analysis software which was to interpret the data (discussed previously). There remain some residual issues with the combined data, concerning the specific frequency resolution – the dissimilar capture hardware can give mismatches in the available sampling rates, clock, and buffer sizes. Some modal solvers can solve for such dissimilar frequency abscissa, although they rely on resampling the data, which may induce tangible error. Mismatched frequency abscissa can potentially see a single mode represented as multiple modes with nominally the same mode shape, separated by one or more discrete frequency increments. Ultimately, the ideal solution is to build a capture tool that unifies clocks, excitation bandwidth and sample frequencies.

### Matching SLDV Test Geometries to FE Models

Accelerometer and SLDV geometries are typically generated by different means. The accelerometer array is located by the considered, deliberate act of attaching individual physical transducers to the test-piece. The SLDV measurement “grid” is usually defined by drawing scanned objects on the calibrated video feed, adding single measurement points, line sections, or polygons to cover areas. For large objects viewed on a relatively low-resolution video feed, the spatial accuracy with which a measurement point can be placed

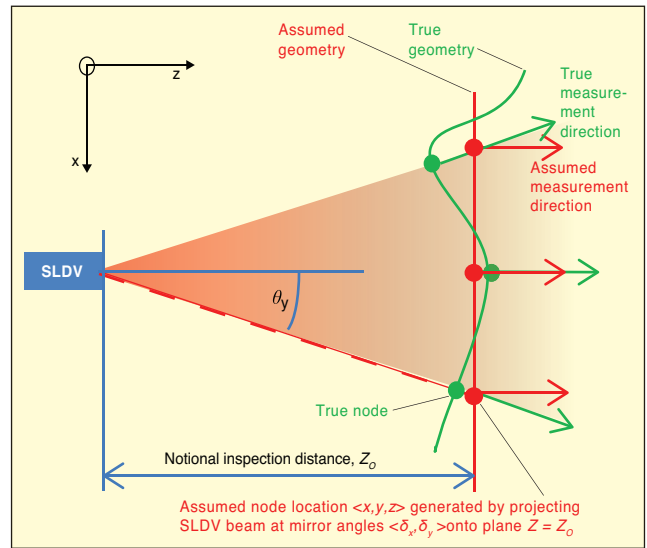


Figure 3. Schematic of assumptions in typical SLDV test geometry without range finding.

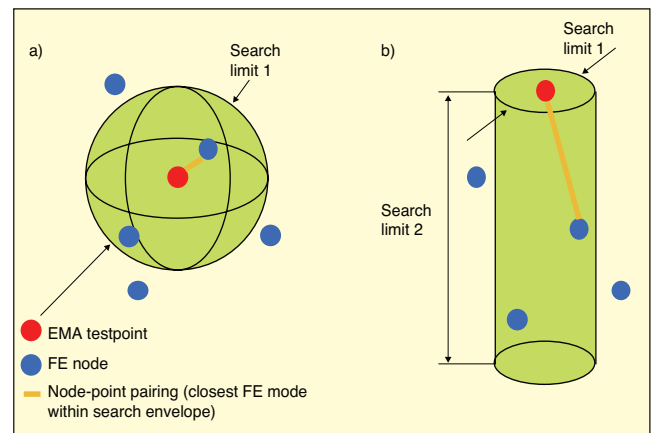


Figure 4. Schematic showing (a) typical FEA/EMA node-point pairing, (b) a simple, improved FEA/EMA node-point pairing method for SLDV data.

will be noticeably coarse. In the case of scanned objects that cover areas, the actual measurement points are usually set to comprise a number of key points around the perimeter of the object, with a number of measurement points in the enclosed area, typically uniformly spaced (rectangular grid, tessellated triangles, etc.) with respect to the pixels of the video feed.

Unless the SLDV has the facility for range-finding, the two-dimensional geometry defined by the pixels in the video feed is the only geometry information available and is often converted into units of measurement by simple scaling. Since the geometry lacks a depth dimension, the geometry is limited to a plane (Figure 3). Further, the velocity measurement is typically considered to be perpendicular to the plane, rather than along the laser beam axis. This places limitations on the test design, since the assumption that the velocity is out of plane could lead to significant inaccuracy in a model correlation.

Accelerometer array geometry is usually fitted to the FE model most easily by simple minimum distance (Figure 4a). There are often small errors in the matching process due to mismatches between the FE and EMA geometries, which are typically corrected more easily for accelerometers simply because there are usually fewer accelerometer measurement points. Since the SLDV data are usually from a single viewpoint, a simple projection along one axis is typically adequate to match the SLDV data to an FE model (Figure 4b), although correction of the measurement angle is necessary if the SLDV measurement axis was deflected significantly.

### Case Study

The UB100X is a University of Bristol test assembly that was designed to represent a highly simplified helicopter tail cone with





Figure 5. Composite photograph showing inspiration for the UB100X structure – the AgustaWestland 159 “Wildcat” tail cone and wing.

wing (Figure 5). The parts of the assembly considered in this article are UB100X-B (Component B), a box structure that represents a simplified helicopter tail-cone, and UB100X-C (Component C), which represents a wing attached by four interference-fit pin joints to UB100X-B. Component B was welded together from aluminium plate and has a number of features: large holes in two opposite faces, heavy flanges at one end, and brackets for attaching Component C. Component C is simply an aluminium plate with the corresponding brackets to component B. The brackets are bolted rigidly to the structure.

### Virtual Testing and Experimental Analysis

The assembled box and wing structure was to be tested using a combination of accelerometers and SLDV, but given the difficulty in representing SLDV measurement locations with current virtual test tools, we decided to consider only the accelerometers and to supplement the accelerometer array with an SLDV test geometry using operator judgement.

First, Component B was considered in the virtual test software without the wing (Component C) attached on the premise that the SLDV can easily measure many points on the attached wing. (usefully the SLDV avoids adding mass and damping to the wing.) Component b was considered in isolation to avoid the confusion of the many aliased modes that would result in the B + C configuration with no degrees of freedom (DOFs) on Component C. However, we acknowledge that this is not ideal, since the modes of B will differ somewhat from the modes of Component B with Component C attached. Note also that it was observed in experimental data taken on the box without the wing, that the model upon which the virtual test was based did not behave with as much symmetry about the longitudinal axis as the genuine article, which explains some of the difficulty with the virtual test. Tests on the box structure alone are omitted here for brevity, but it is noteworthy that the box-only model could not be validated for updating, while the B+C model was adequate for updating.

The FE mesh comprised TET10 elements and was generated automatically from a CAD model using MSC PATRAN. Using automated DOF placement, we found it extremely difficult to place the DOFs for both unique determination of modes and for human visualisation of the modes, with the software tending to cluster the available DOFs at one end of the box (Figure 6a). This test geometry is also found to be difficult to copy onto the genuine structure, and it would be easy to make an error in attaching, wiring and cataloging the accelerometers, since the test geometry is non-intuitive to the operator. This automated placement was achieved using an oft-used means of automatically placing a large number of DOFs (80 in this case) using normalized modal displacement (NMD) and then reducing the number of DOFs (here to 25) by considering the effect on the MAC.

A test geometry with the same pattern of DOFs applied to each panel surface was manually defined in the virtual test software (see Figure 6b). This geometry was found to give minimal aliasing of the mode shapes over the frequency range of 0-250 Hz (see autoMAC matrix, Figure 7), and the modes that correlate due to aliasing are

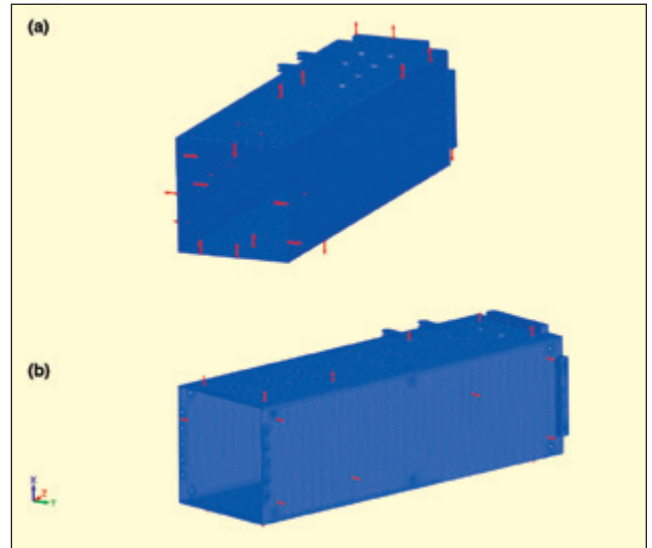


Figure 6. UB100X-B accelerometer test geometry from (a) automated DOF placement using normalised modal displacement and DOF reduction using MAC, (b) operator intuition.

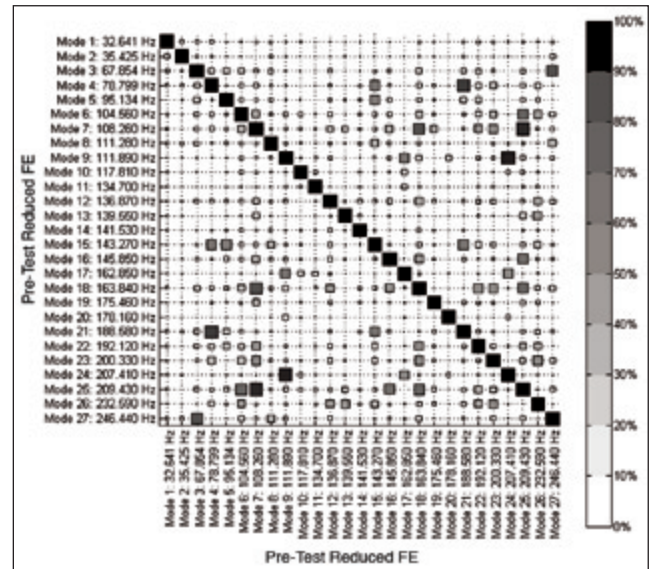


Figure 7. AutoMAC matrix for prototype test geometry on UB100X-B shown in Figure 6b.

observed to occur at dissimilar frequencies.

The complete UB100X B+C model was meshed, again from a CAD model using TET10 elements in MSC PATRAN, with the pin-joints considered rigid (the whole assembly was effectively monolithic). The experimental modal analysis was performed using a Polytec PSV-300 SLDV system and an LMS SCADAS to control the accelerometer capture. Figure 8 is a photograph of the experimental configuration.

The experiment was performed using a single exciter, which was a necessary concession to the capabilities of the SLDV system (note that newer systems can perform MIMO). The combined accelerometer and SLDV test geometry is shown in Figure 9. An autoMAC matrix for a posteriori reduction of the FE model using the test geometry points is shown in Figure 10. This autoMAC matrix is observed to be largely well conditioned, although there are some significant off-diagonal terms. Examples of the aliased modes are given in Figure 11, typified by similar behavior on the faces that the SLDV can observe, but various symmetric and non-symmetric shapes on the faces of the box section that the SLDV could not be observed.

Note that with better integration of the SLDV into the virtual test, this autoMAC matrix could have been found a priori and a better-informed test performed. The SLDV was approximately perpendicular to the areas on which it is measured (the wing and

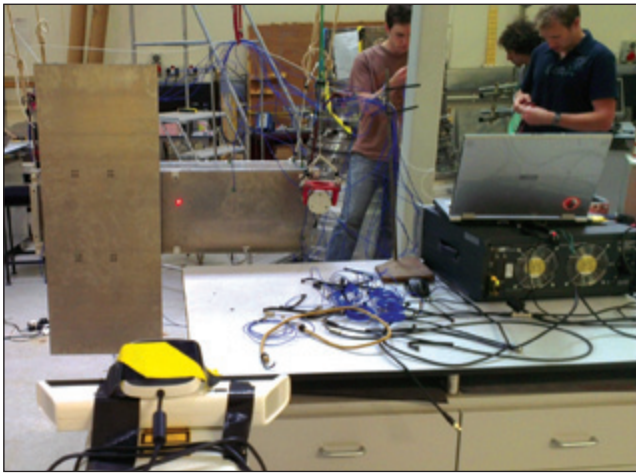


Figure 8. Experimental setup.

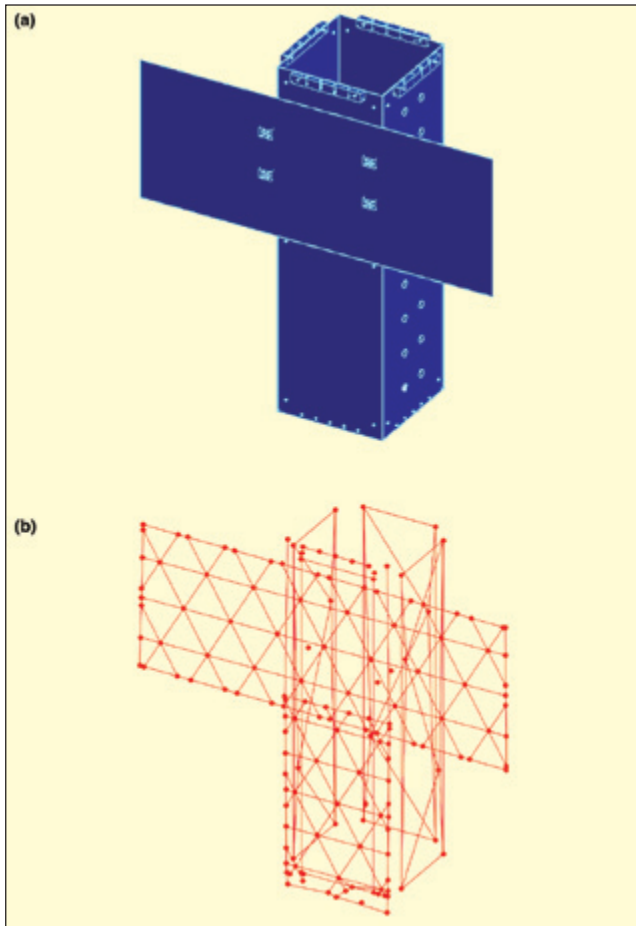


Figure 9. Test structure UB100X Components B and C, (a) FE model, (b) EMA test geometry.

some of one face of the box section) largely as a convenience to aid assimilation of the datasets, but a location of the SLDV head that also gave a view of the top of the box would have significantly reduced the instances of aliased modes.

### Experimental Modal Analysis and Model Correlation

The experimental SLDV and accelerometer FRF data were combined in a MathWorks MATLAB program, performing the functions described earlier and outputting a master universal file. The combined dataset was imported once more into LMS Test.lab, and a modal solution was found. The experimental mode shapes were exported, again as a universal file, into Dynamic Design Solutions FEMtools for correlation and model updating.

Despite the relative simplicity of the component B+C model and the previous poor results from a Component B-only correlation,

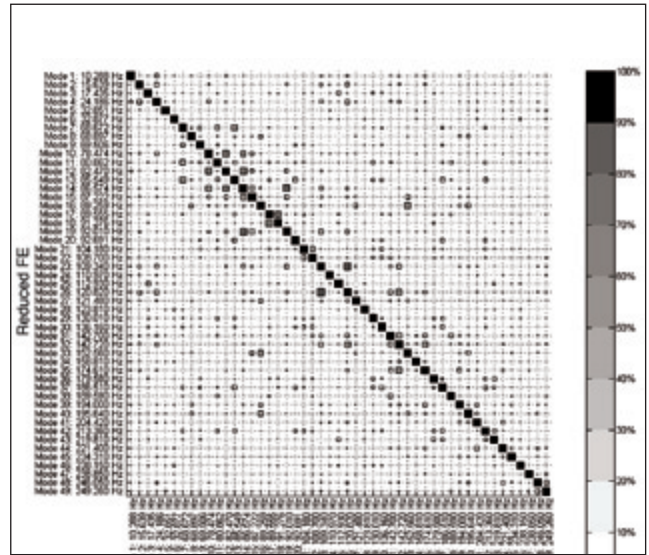


Figure 10. A posteriori autoMAC matrix for the UB100X-B+C model shown in Figure 9a, reduced using EMA points in Figure 9b.

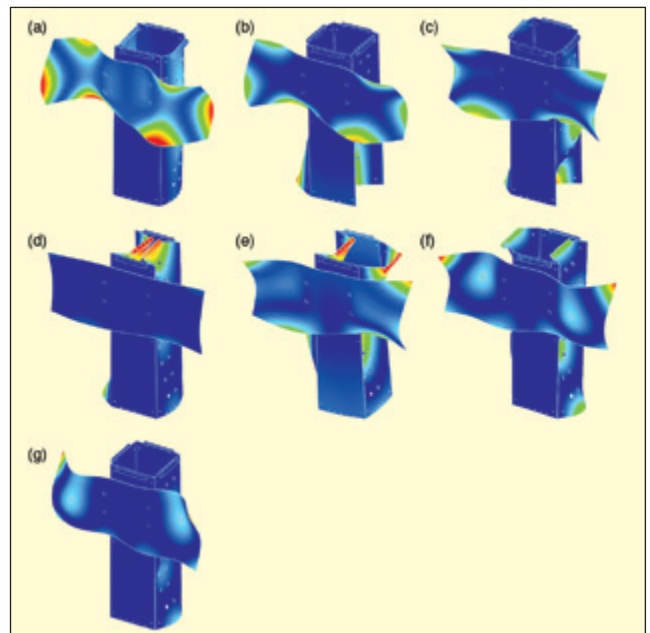


Figure 11a-g. FE modes 10, 12, 14, 15, 19, 23, 26 respectively; these FE modes are given as examples of high off-diagonal mode pairs in autoMAC matrix in Figure 10. The reduced geometry that aliased these mode shapes is given in Figure 9b, from which it is clear that while the SLDV allows adequate description of these high-order mode shapes on the wing, critically, the sides of the box are inadequately characterized.

the correlation between the test data and non-updated model were observed to be mostly good, albeit with some high off-diagonal terms in the MAC matrix (Figure 12) caused by aliasing of modes in areas the SLDV could not measure. The FE and EMA modes were paired based on a minimum MAC of 50%, with no repeated pairings (each mode could only be paired once), and no restriction between the difference in frequency of the modes. This relative lack of constraint and relatively low minimum MAC is acknowledged to be potentially sub-optimal, but it can be instructive to see how well the FE and EMA agree with minimal intervention.

The UB100X B+C structure was observed to exhibit effectively no local modes; the box has inherent symmetries, and as a welded assembly is assumed to have a fairly uniform mechanical impedance (distributed stiffness). Considered individually, both the box and wing feature many modes in the frequency range of interest (0-250 Hz), so it is not surprising that when considered as a system (B attached to C), all modes see some participation from both components. In the case of the UB100X B+C assembly, the lack of



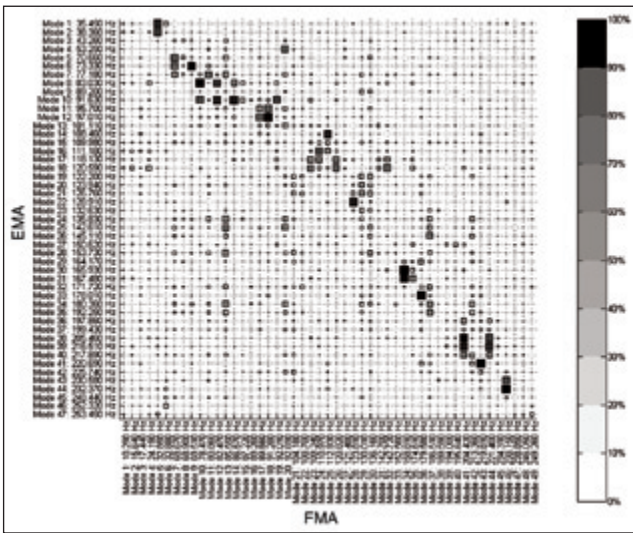


Figure 12. FEA/EMA MAC Matrix for UB100X B+C structure before model updating.

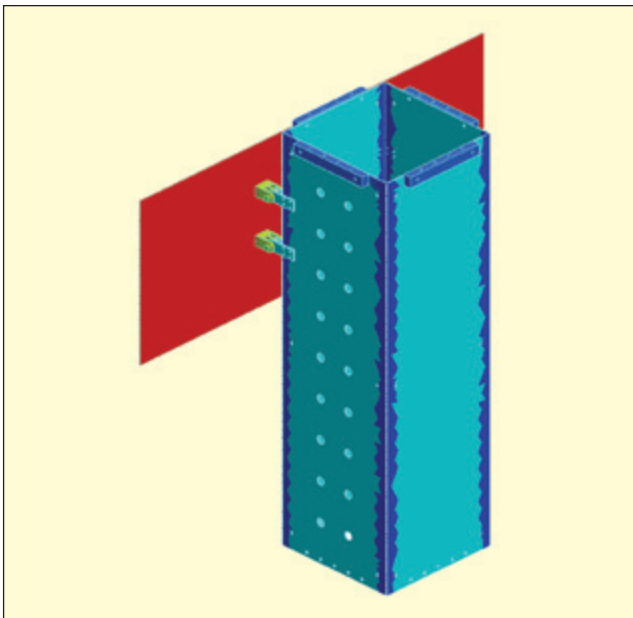


Figure 13. FE model of Components B (box section) and C (wing), broken into subsets: wing, brackets, pins, welds, flanges, bulk (remainder of Component B); parameter updating for density and Young's modulus based on allowing individual materials for each of these subsets are given in Table 1.

local modes instead saw the spatial resolution advantage of the SLDV translated into being able to match a large number of EMA global modes to the FE, namely 20 pairs.

### Model Updating

To explore the influence of the SLDV measurements on the model updating process, multiple model updates were trialled with the complete EMA dataset and a reduced EMA dataset representative of the spatial resolution that could be reasonably achieved with accelerometers. In the reduced EMA dataset, there were six SLDV DOFs left on the wing (corners plus mid-points), which gave a total of 31 DOFs (including a force reference on the driving point that would populate a 32-channel acquisition system). The model updating was performed in several different ways, as is often the case when trying to understand the sensitivity of a model to changes in parameters, as explained in the following sections. The common settings between all updates were mass-density  $\rho$  and young's modulus  $E$  and were parameterized with no constraint on the amount they could be varied. The responses were a target mass and to optimize the frequencies and MAC for the paired modes. Updating was stopped when the correlation criterion fell below a certain level or no improvement was seen

between model iterations.

**Model Updating Using Global Parameters of Component Subsets.** The first updating method that was trialled was to define subsets of the B+C structure, then allow the parameters (density and Young's modulus) to vary globally for each subset. The subsets are shown in Figure 13. The idea behind this parameterization was to identify which components of the model were not representative of the real structure. The structure was fabricated from sheet and billet aluminium, so it seems implausible that these properties should vary much locally, except at joints. There remains a question over the properties of the welds, but these do appear to be of a very high quality so are assumed to be similar to the parent aluminium structure. This means of parameterization is appealing, because if such a model update can be validated, the component parts of the model are each described by a single material and not many materials per component.

The results from the updating are shown in Table 1. The effect of reducing the number of measurement points on the structure was significant, with the complete dataset strongly altering the properties of the wing (Component C), the welds, and the flanges, while the reduced dataset saw the strong alteration of the welds, the brackets and the pins. The results for the reduced dataset appear more plausible, since it identifies the joints between the wing and box section. The complete dataset saw the mass of the wing more than double (with the increase in stiffness presumably compensating for the otherwise reduced resonant frequencies), which is highly unrealistic.

**Model Updating Using Local Parameters.** A second round of updating was performed, this time allowing local parameterization for all FE nodes. In Figures 14 and 15, the updated model is shown for the complete and reduced datasets respectively. As was observed in the updating using global parameters on subsets of the model, the updating results vary significantly for the complete and reduced datasets. While the results from the two datasets bear a resemblance, the reduced dataset sees greater local variation and contrast in the density and Young's modulus parameters. This is particularly apparent on the wing section, in which the Young's modulus map sees strong increases around all four attachment points to the box section. "shadows" of the paired modes are apparent in the local variations of the parameters, and given that different numbers of modes could be paired for the two datasets, this accounts for some of the difference in the updating results.

A further model update was performed, taking the updated models and then allowing local parameterization as described above. The underlying idea was that the first round of updating using global parameters of subsets should have given a better model to start from, with the local updating then requiring fewer iterations and less strong local variation of the parameters to converge. Again,

Table 1. Values for density and Young's modulus after model updating based on component subsets; complete EMA dataset and reduced version of the same dataset were considered.

	$\rho$	$\Delta \rho/\rho, \%$	$E$	$\Delta E/E, \%$
<b>Starting Values</b>	<b>2700</b>	—	<b>6.90E+10</b>	—
			<b>Complete Dataset</b>	
Component B (bulk)	2556	-5.33	7.06E+10	2.32
Component C	6303	133.44	1.17E+11	69.86
Welds	298	-88.96	4.89E+10	-29.13
Brackets	2764	2.37	9.16E+10	32.75
Pins	2785	3.15	8.80E+10	27.54
Flanges	2059	-23.74	5.40E+09	-92.17
			<b>Reduced Dataset</b>	
Component B (bulk)	2885	6.85	6.99E+10	1.30
Component C	1883	-30.26	5.84E+10	-15.36
Welds	1670	-38.15	3.56E+10	-48.41
Brackets	10911	304.11	4.44E+09	-93.57
Pins	3459	28.11	1.20E+11	73.48
Flanges	2836	5.04	7.15E+10	3.62

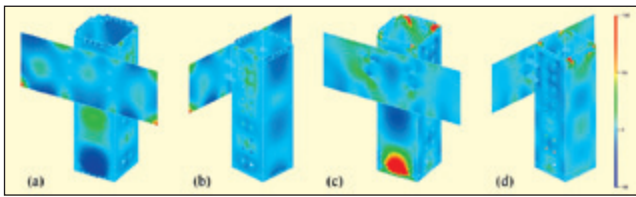


Figure 14. UB100X model after update using local parameters; change in (a), (b) density; (c), (d) Young's modulus.

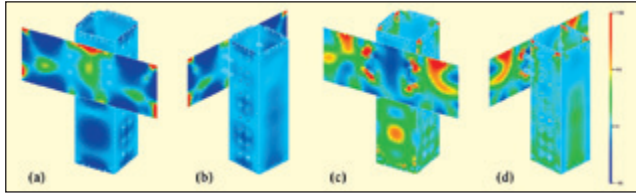


Figure 15. UB100X model after update using local parameters on the reduced test geometry; change in (a), (b) density; (c), (d) Young's modulus.

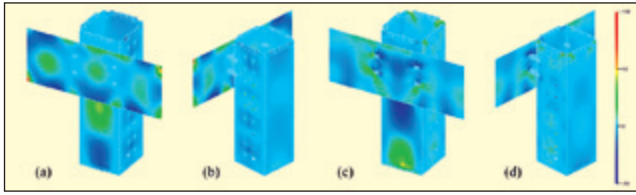


Figure 16. UB100X model after update using global subsets, then local parameters; change in (a), (b) density; (c), (d) Young's modulus.

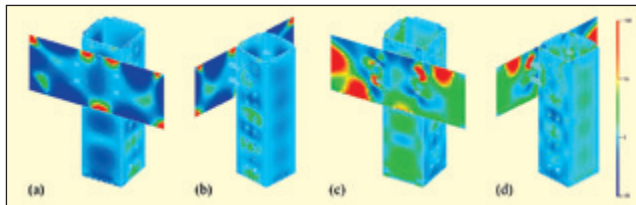


Figure 17. UB100X model after update using global subsets, then local parameters on reduced test geometry; change in (a), (b) density; (c), (d) Young's modulus.

the model updating was performed twice, first on the complete and secondly on the reduced datasets, with the results shown in Figures 16 and 17, respectively. This two-stage approach appears to have lessened the amount of local updating on Component B, though Component C appears much the same, with the patterns in the maps of density and Young's modulus both seeming to indicate some deficiency in the modeling of the joints.

The two-stage approach applied to the reduced dataset yielded results different to both local-only updating of the complete dataset (Figure 14), and local-only updating on the reduced dataset (Figure 15). The strong and well-defined updates around the Component C joints in the local-only update of the reduced model are not as clear, and there is more local variation of the parameters on the sides of Component B.

The natural frequencies for the paired modes for each of the updating trials discussed in this article are given for the complete and reduced datasets in Figure 18. From this plot it is clear that the mode pairing for the complete dataset (blue points) is better than for the reduced dataset (red points). This is not surprising, since the reduced dataset gives an increase in instances of aliased modes. Note that a restriction was placed on the frequency difference allowed in mode pairing for the reduced dataset (no greater than 50%), while no restriction on frequency was necessary for the complete dataset.

The lower numbers of paired modes for the reduced dataset and higher numbers of spurious pairings strongly supports use of a SLDV in this application. The small number of poor mode shape pairings observed with the complete dataset may have been improved by locating the SLDV in a different position relative to the test structure so that multiple faces of Component B could be observed.

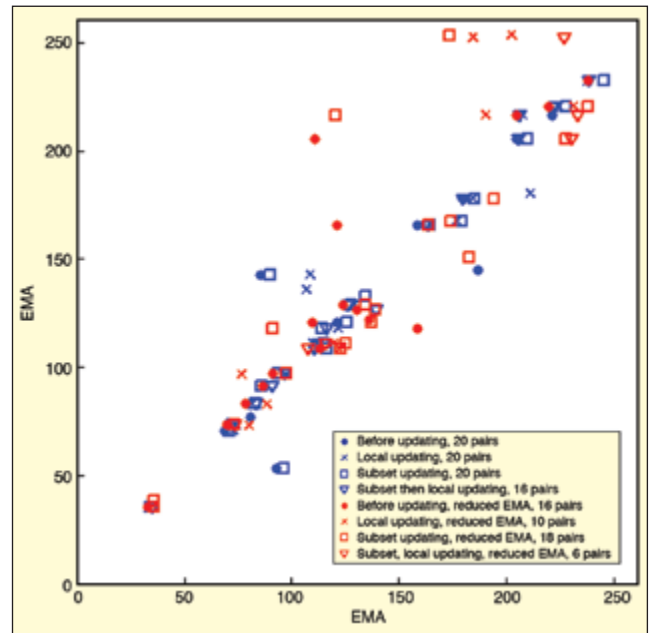


Figure 18. Frequency-frequency plot for paired mode shapes ( $MAC \geq 50\%$ ); no restriction on frequency difference was set for complete dataset, but maximum frequency difference of 50% was set for reduced dataset to minimise pairing of aliased modes.


## Conclusions

In this article, various means of performing modal testing using SLDVs were discussed, with particular attention on the challenges encountered in importing measured data into existing modal analysis software packages. A case study of the application of a hybrid SLDV and accelerometer test geometry was demonstrated, and the correlation with a basic FE model through to high-order modes was shown to be extremely good. The SLDV was shown to be a useful tool for modal analysis, although the line-of-sight limitation of such a device must be considered when trying to characterize the structural dynamics of a three-dimensional structure. Development of virtual testing tools to optimize use of a SLDV is highly desirable and would significantly increase the benefit in the use of SLDVs for modal analysis.

Various model-updating trials were explored, including use of a reduced number of degrees of freedom. We showed that the use of large numbers of degrees of freedom increased the number of model and test mode shapes that could be paired and reduced instances of spatial aliasing. The updated model was clearly affected by change in the number of degrees of freedom, although the merit in the increased number of measurement locations is difficult to qualify and is likely application specific.

Interpreting results from model updating is often difficult, and the model updating process itself will – for better or worse – converge toward a solution based solely on the parameters, responses and metrics for correlation defined by the operator. However, the option to match the response of the finite-element model to an experimental measurement at a greater number of locations as afforded by use of SLDV often seems appealing.

## References

1. S. Rothberg, "Numerical Simulation of Speckle Noise in Laser Vibrometry," *Applied Optics*, Vol. 45, pp. 4523-4533, 2006.
2. M. Sraric and M. Allen, "Experimental Investigation of the Effect of Speckle Noise on Continuous Scan Laser Doppler Vibrometer Measurements," *Proceedings of IMAC XXVII*, Orlando, Florida, 2009.
3. AIVELA, Ancona, 2012.
4. D. Ewins, *Modal Testing 2*, Research Studies Press Ltd., Hertfordshire, England, 2000.
5. University of Cincinnati, SDRL, "Universal File Formats for Modal Analysis Testing," <http://www.sdrl.uc.edu/universal-file-formats-for-modal-analysis-testing-1/universal-file-formats-for-modal-analysis-testing>.
6. K. S. Arun, T. S. Huang and S. D. Blostein, "Least-Squares Fitting of Two 3D Point Sets," *IEEE Transactions on Pattern Analysis and Machine Intelligence*, Vol. 9, No. 5, pp. 698-700, 1987. 

The author can be reached at: [benweekes@gmail.com](mailto:benweekes@gmail.com).